Nat Hazards (2014) 71:837–850
DOI 10.1007/s11069-013-0934-1

ORIGINAL PAPER

A new procedure to best-fit earthquake magnitude probability distributions: including an example for Taiwan

J. P. Wang · Yih-Min Wu · Duruo Huang · Su-Chin Chang

Received: 5 June 2012 / Accepted: 28 October 2013 / Published online: 6 November 2013

Abstract Since the year 1973, more than 54,000 $M_w \geq 3.0$ earthquakes have occurred around Taiwan, and their magnitude–frequency relationship was found following with the Gutenberg–Richter recurrence law with *b* value equal to 0.923 from the least-square calculation. However, using this *b* value with the McGuire–Arabasz algorithm results in some disagreement between observations and expectations in magnitude probability. This study introduces a simple approach to optimize the *b* value for better modeling of the magnitude probability, and its effectiveness is demonstrated in this paper. The result shows that the optimal *b* value can better model the observed magnitude distribution, compared with two customary methods. For example, given magnitude threshold = 5.0 and maximum magnitude = 8.0, the optimal *b* value of 0.835 is better than 0.923 from the least-square calculation and 0.913 from maximum likelihood estimation for simulating the earthquake's magnitude probability distribution around Taiwan.

Keywords Earthquake magnitude probability · *b* value · Optimization · Taiwan

J. P. Wang (✉) · D. Huang
Department of Civil and Environmental Engineering, Hong Kong University of Science and Technology, Clear Water Bay, Hong Kong
e-mail: jpwang@ust.hk

D. Huang
e-mail: drhuang@ust.hk

Y.-M. Wu
Department of Geosciences, National Taiwan University, Taipei, Taiwan
e-mail: drymwu@ntu.edu.tw

S.-C. Chang
Department of Earth Sciences, The University of Hong Kong, Pokfulam, Hong Kong
e-mail: suchin@hku.hk

1 Introduction

Earthquake prediction is controversial given our limited understanding of the uncertain earthquake process (Geller et al. 1997; Mualchin 2005). Some practical solutions including seismic hazard analysis and earthquake early warning are employed for earthquake hazard mitigations (Geller et al. 1997; Wu and Kanamori 2005, 2008; Wang et al. 2012a). Probabilistic Seismic Hazard Analysis (PSHA), referred to as the Cornell–McGuire method (Cornell 1968; McGuire and Arabasz 1990), is one of the representative methods for seismic hazard assessment. Many PSHA case studies have recently been conducted (Anbazhagan et al. 2009; Sokolov et al. 2009; Mezcua et al. 2011; Rafi et al. 2012; Wang et al. 2013), and technical references are now prescribing the use of PSHA for developing earthquake-resistant designs for critical structures (U.S. Nuclear Regulatory Commission 2007).

The purpose of PSHA is to account for the uncertainties of earthquake magnitude, location and motion attenuation (Kramer 1996). As a result, the magnitude probability distribution is one of the PSHA's inputs. Nowadays, the McGuire–Arabasz (M–A) algorithm (1990) is the customary approach to develop such a magnitude function. (The mathematical expressions of this algorithm are detailed in one of the following sections.) For instance, using b values equal to 0.8 and 1.0, the magnitude probability distributions from a PSHA benchmark example are shown in Fig. 1 (Kramer 1996). These distributions account for the magnitude uncertainty in the PSHA calculations.

The M–A algorithm is a function of the b value, which is the slope in the Gutenberg–Richter (G–R) relationship, a regression model between the logarithm of earthquake rate ($\log \lambda_{M \geq m^*}$) and magnitude of exceedance (m^*). (More details about the G–R recurrence law are also given later.) The b value or the slope can be obtained with the fundamentals of regression analysis governed by the least-square (LS) algorithm. Another option for estimating the b value is to use maximum likelihood estimation (MLE) (Weichert 1980).

Apart from its applications, the b value alone does not contain clear physical meaning to earthquake physics. Statistically speaking, a region with b value $= 0.5$ has a higher percentage of large earthquakes compared to a region with b value $= 1.0$. But what causes b value $= 0.5$ in this region is difficult to explain. Further research should be pursued to develop a better understanding of earthquake physics and the G–R recurrence law, as well as the possible physical indications of the b value to earthquakes, but it is not within the scope of this study.

This study aims to present a new procedure to calibrate the b value for better modeling of magnitude probability distributions with the customary M–A algorithm. We used the earthquake data around Taiwan as an example to demonstrate this new procedure, with two customary b value calculations also employed for comparison.

2 Gutenberg–Richter recurrence law

The Gutenberg–Richter (G–R) recurrence law was first proposed with earthquake data from California (1944). It suggests a linear correlation between $\log \lambda_{M > m^*}$ and m^* from regression analyses:

$$\log(\lambda_{M \geq m^*}) = a - bm^* \tag{1}$$

where a and b (also known as the a value and b value) are referred to as the G–R recurrence parameters.

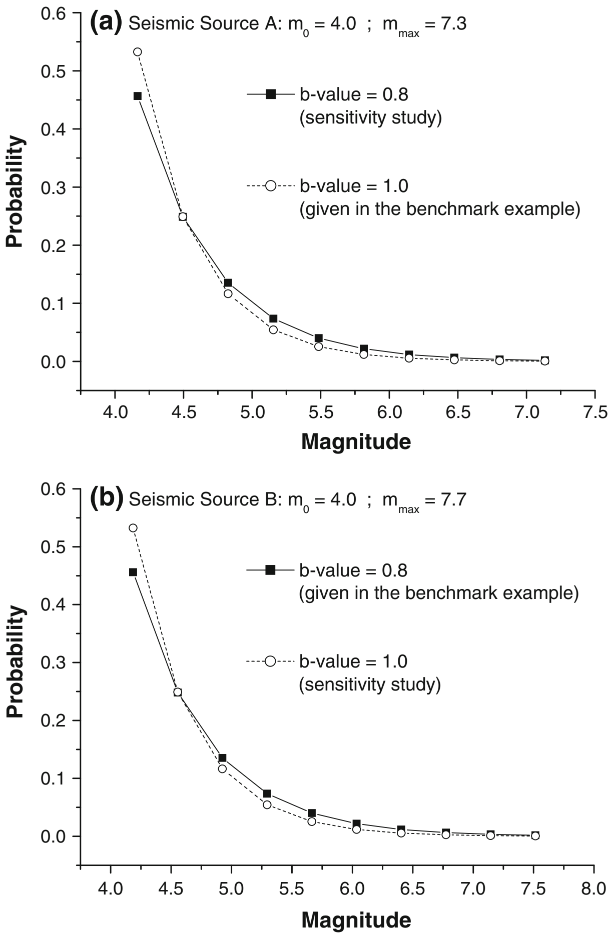

Fig. 1 *b* values and magnitude probability distributions in a benchmark PSHA example: **a** Seismic Source A with $m_0 = 4.0$ and $m_{\max} = 7.3$, and **b** Seismic Source B with $m_0 = 4.0$ and $m_{\max} = 7.7$. Note that the magnitude distributions were calculated with the McGuire–Arabasz algorithm given in Eq. 3

Figure 2 shows the locations of more than 54,000 $M_w \geq 3.0$ earthquakes, which have occurred since the year 1973 around Taiwan, approximately within the region bound by longitude 119°E to 123°E and latitude 21.5°N to 25.5°N. The largest magnitude recorded was around M_w 7.95, so that the maximum magnitude used in the following calculations was taken as 8.0. This seismicity or earthquake catalog has been employed previously for earthquake statistics studies, including the probability distribution of the annual maximum earthquake (Wang et al. 2011), the probability distribution of PGA (Wang et al. 2012b), and the earthquake's temporal distribution around Taiwan (Wang et al. 2013). More attributes of this catalog, such as magnitude thresholds and declustering methods, were also detailed in those previous studies.

Figure 3 shows the G–R relationship for the seismicity around Taiwan, with *a* value and *b* value equal to 5.831 and 0.923, respectively, given a magnitude increment of 0.5 employed. The model's R^2 is 0.996, validating the effectiveness of using this empirical relationship for earthquakes around Taiwan.

Nevertheless, the regression model is not a perfect fit to earthquake data. For example, at $m^* = 3.0$, the observed mean annual rate is higher than the model's prediction, and the situation is opposite at $m^* = 5.0$ (see Fig. 3). To be more specific, at $m^* = 3.0$, the model's prediction of $\log \lambda_{M \geq 3.0}$is equal to 3.062 (=5.831–0.923 × 3), less than 3.166

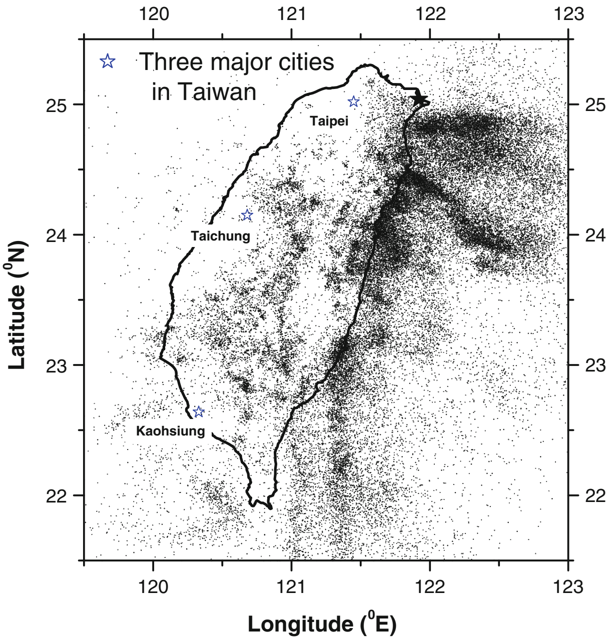

Fig. 2 Spatial distribution of more than 54,000 $M_w \geq 3.0$ earthquakes around Taiwan since 1973

from observation. After "de-log", the observed and expected annual rates are 1,466 and 1,153 per year. It is somewhat surprising to see this substantial difference given a nearly perfect regression model ($R^2 = 0.996$) between log $\lambda_{M \geq m^*}$ and m^*. But owing to the nature of mathematics, after performing "de-log" on $\log(N_{M \geq m^*})$, the difference between observed and expected $N_{M \geq m^*}$ can be substantially amplified.

3 Magnitude probability distribution

McGuire and Arabasz (1990) developed the magnitude probability function utilizing the concept of conditional probability, later becoming a customary method used in earthquake-related analyses, such as PSHA, when the uncertainty of earthquake magnitude is taken into account (Kramer 1996). The purpose of this development is to calculate the ratio of earthquakes of interest (i.e., $m_1 \leq M < m_2$) to total earthquakes (i.e., $m_0 \leq M < m_{\max}$), as follows:

$$\Pr(m_1 \leq M < m_2 | m_0 \leq m_1, m_2 \leq m_{\max}) = \frac{N(m_1 \leq M < m_2)}{N(m_0 \leq M < m_{\max})}, \tag{2}$$

where m_0 and $m_{\max}$ are referred to as magnitude threshold and maximum magnitude. Combining Eqs. 1 and 2, the calculation of magnitude probability becomes:

$$\begin{aligned}\Pr(m_1 \leq M < m_2 | m_0 \leq m_1, m_2 \leq m_{\max}) &= \frac{10^{a-bm_1} - 10^{a-bm_2}}{10^{a-bm_0} - 10^{a-bm_{\max}}} \\ &= \frac{10^{-bm_1} - 10^{-bm_2}}{10^{-bm_0} - 10^{-bm_{\max}}}\end{aligned} \tag{3}$$

As a result, the M–A algorithm is governed by a single b value. With $m_0 = 4$, $m_{\max} = 8$, and $b = 0.923$ calibrated from the earthquake data with the LS calculation,

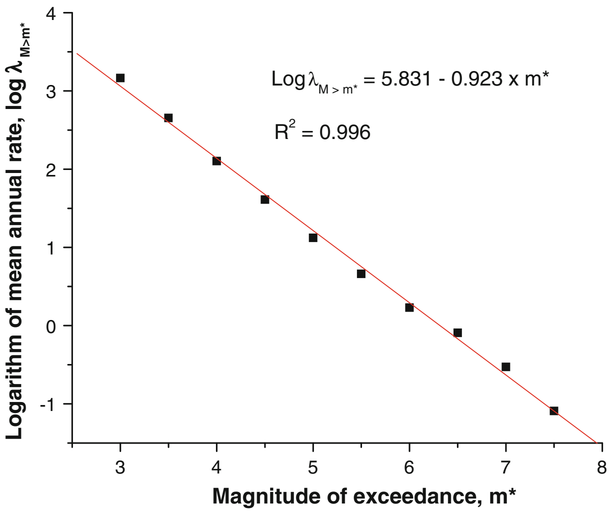

Fig. 3 The Gutenberg–Richter empirical relationship for the seismicity around Taiwan (Fig. 2); note that the mean annual rate was calculated with the total events divided by the duration of observation

Fig. 4 shows the expected and observed magnitude distributions. The model prediction and observation are found in a good agreement. To quantify the level of fitting, we calculated the χ^2 value from the following expression (Ang and Tang 2007; Devore 2008):

$$\chi^2 = \sum_{i=1}^{n} \frac{(e_i - o_i)^2}{e_i}, \tag{4}$$

where n is the number of data points; e_i and o_i are the expected and observed values of the i-th data point in the regression. In this case (Fig. 4), the χ^2 value is calculated at 0.012. Note that a lower χ^2 value indicates a better curve fitting between prediction and observation.

4 *b* value through maximum likelihood estimation

The other customary procedure to estimate the *b* value is through maximum likelihood estimation (MLE). Assuming earthquake occurrence in time follows the Poisson model, the likelihood function was developed with observed earthquakes. Then, the MLE *b* value can be determined by solving this likelihood function. Following the numerical procedure suggested by Weichert (1980), the MLE *b* value was calculated at 0.994 for the same seismicity. With it, Fig. 5 shows the fitting between the model's prediction and the same observational data. Compared to the LS *b* value of 0.923, the MLE *b* value of 0.944 improves the fitting by approximately 20 %.

5 The new optimal *b* value for the modeling of magnitude probability

We propose a procedure to search for a better *b* value that can further improve the modeling of magnitude probability distributions from the same M–A algorithm (i.e.,

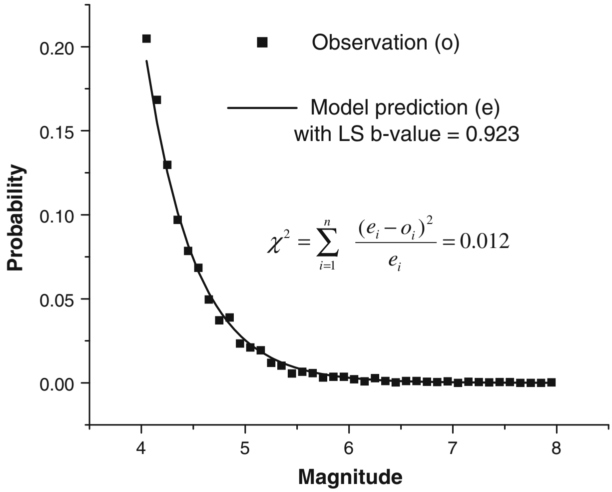

Fig. 4 Observed and expected magnitude probabilities with the least-square (LS) b value of 0.923. Throughout the magnitude range from 4.0 to 8.0, the level of fitting characterized by the χ^2 value is equal to 0.012 (the lower the value, the better the fitting.)

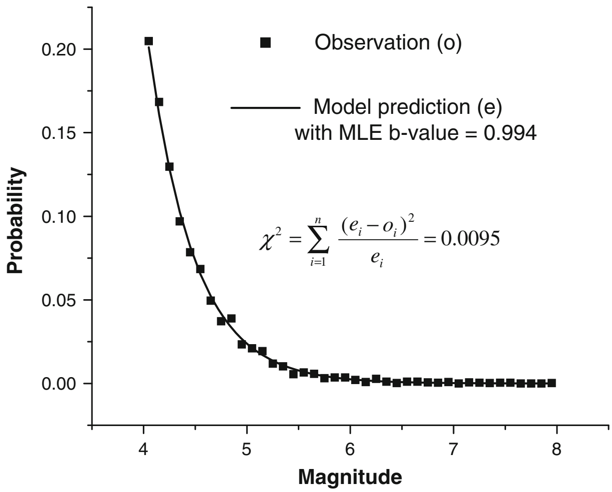

Fig. 5 Observed and expected magnitude probabilities with the MLE b value of 0.994. Throughout the same magnitude range as Fig. 4, the χ^2 value was reduced to 0.0095, from 0.012 using the LS b value of 0.923

Eq. 3). The procedure used is simply trial-and-error. With a series of b values being tested, the one accompanying the lowest χ^2 value is considered the optimal value. Fig. 6 shows the optimizing with the bowl-shaped distribution between b values, and χ^2 values for the case shown in Figs. 4 or 5. An optimal b value indeed comes to existence at the trough of the curve with a minimized χ^2 value. Likewise, Fig. 7 shows the fitting between observation and expectation with the optimal b value = 0.975, which provides another 5 percent improvement for this curve fitting over the use of the MLE b value of 0.944.

6 Parametric study

The results demonstrated in Figs. 4, 5, 6, 7 are under a specific boundary condition, i.e., $m_0 = 4.0$ and $m_{max} = 8.0$. Following the same analysis, we conducted parametric studies given three more boundary conditions (different magnitude thresholds with the same maximum magnitude of 8.0), and the respective results are shown in Fig. 8. Similarly, the optimal b value pertaining to the lowest χ^2 value can be found on the curves. Although in some cases (e.g., Fig. 8a), the optimal value is very close to the LS or MLE value, it fits the observation better than the two regardless. Figure 9 shows the magnitude probability distributions with three different b values given these magnitude thresholds, and Table 1 summarizes the parameters for each case.

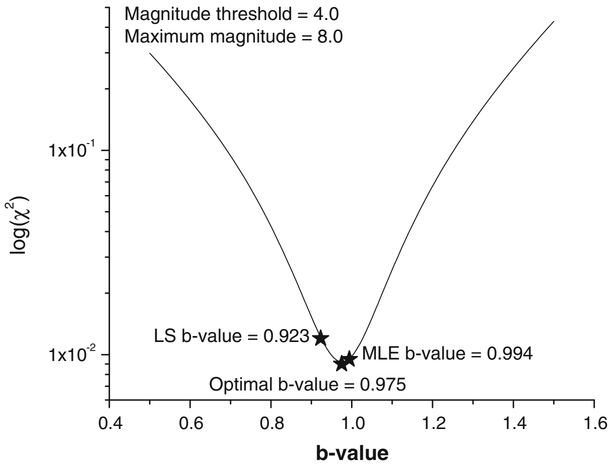

Fig. 6 Relationship between b values and χ^2 values fitting the observed magnitude probability distribution (Figs. 4 or 5). Regardless of the level of difference, the optimal b value of 0.975 is associated with the minimized χ^2 value

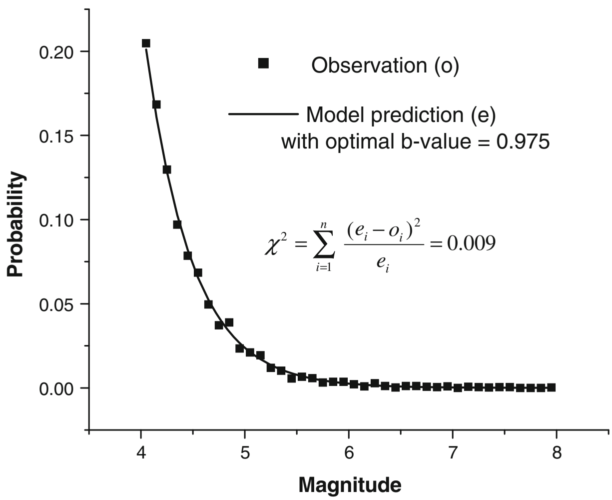

Fig. 7 Observed and expected magnitude probabilities with the optimal b value of 0.975; the χ^2 value was further decreased to 0.009, better than using LS or MLE b value (Figs. 4 and 5)

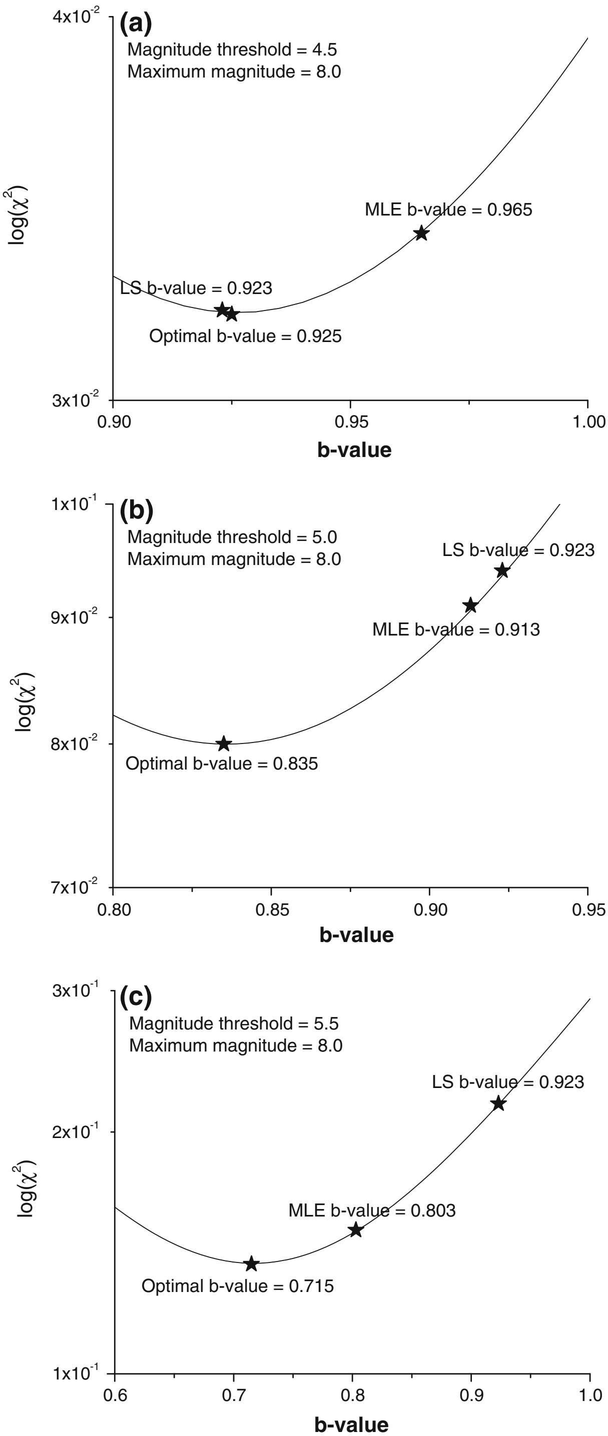

Fig. 8 Parametric studies for three additional magnitude thresholds; likewise, optimal *b* values outperform the two from the LS and MLE calculations, regardless of the level of difference

Figure 10 shows the empirical relationship between the magnitude thresholds and optimal b values from the four analyses. The correlation between the two variables follows a second-order polynomial regression with R^2 of 0.996:

$$b = 0.819 + 0.180m_0 - 0.035m_0^2 \pm 0.01 \tag{5}$$

where the error term ± 0.01 denotes the model's standard deviation. As the G–R law, this empirical model suggests a best-fit correlation between the two variables from earthquake data around Taiwan, without indicating the physical relationship between them. The purpose of such an empirical relationship is to provide a fast estimate of b values for a better simulating of earthquake magnitude distributions around Taiwan, given a magnitude threshold of interest.

It is understood that there are many other combinations in the magnitude threshold and maximum magnitude, but such an optimization is applicable to any set of boundary conditions. In other words, the purpose of using those m_0 and m_{max} values in the demonstrations is to help describe and explain the problem targeted in this study.

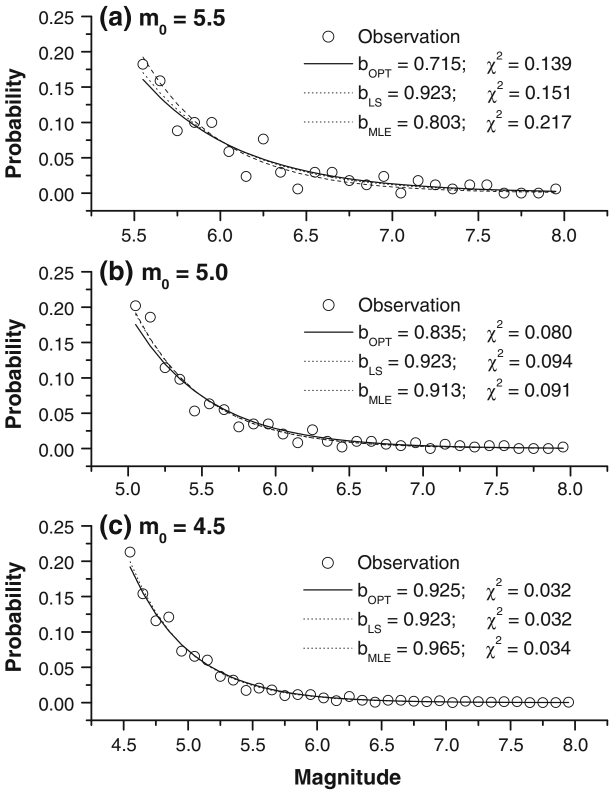

Fig. 9 Observed and expected magnitude probabilities using three b values in the M–A calculation; regardless of the improvement, the optimal b value fits the observation better than those from the two customary methods

Table 1 Summary of *a* values, *b* values, and the corresponding χ^2 values in the modeling of the observed magnitude probability distributions

Methods	Parameters/values	Magnitude threshold m_0			
		4.0	4.5	5.0	5.5
Least square	*a* value	5.831	5.831	5.831	5.831
	b value	0.923	0.923	0.923	0.923
	χ^2 value	0.012	0.032	0.094	0.217
MLE	*a* value	6.080	5.954	5.687	5.088
	b value	0.994	0.965	0.913	0.803
	χ^2 value	0.009	0.034	0.091	0.151
New procedure	*a* value	6.00	5.77	5.30	4.79
	b value	0.975	0.925	0.835	0.750
	χ^2 value	0.009	0.032	0.080	0.137

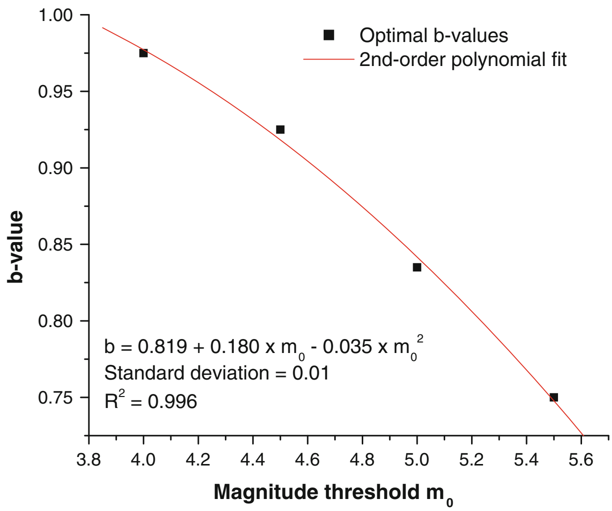

Fig. 10 The empirical relationship between optimal *b* values and magnitude thresholds, providing a fast estimate of *b* values to better modeling of the observed magnitude probability distribution around Taiwan, given a magnitude threshold of interest

7 Conjugate *a* value

With the optimal *b* value being calibrated, its conjugate *a* value can be back-calculated with the observed annual rate, denoted as $\tilde{N}$. Reorganizing Eq. 1, the optimal *a* value (a_{opt}) becomes

$$\begin{aligned} \log(\tilde{N}_{M \geq m_0}) &= a_{\text{opt}} - b_{\text{opt}} m_0 \\ \Rightarrow a_{\text{opt}} &= \log(\tilde{N}_{M \geq m_0}) + b_{\text{opt}} m_0 \end{aligned} \tag{6}$$

As a result, the conjugate pair can match the observed rate $\tilde{N}_{M \geq m_0}$through the G–R law, because it is exactly used for this back calculation. Figure 11 shows the predicted and observed annual earthquake rates for the four demonstrations. Using the least-square parameters, the predicted rates are different from observation. On the other hand, the conjugate algorithm matched to the observed rate as the boundary condition was used to solve the conjugate *a* value.

8 Discussions

8.1 Which *b* value should be adopted?

Input characterization is critical when it comes to an analysis. When input values are the products of curve fitting without physical laws applied, it is preferred to use the one that can fit the observation the best. With this in mind, we will choose the optimal *b* value to calculate magnitude probability distributions, and use the conjugate value to compute annual earthquake rates. But for a study specifically prescribing the G–R law to describe a magnitude–frequency relationship like Fig. 3, we will employ the least-square *b* value because, by the nature of mathematics, there is not a single set of values that can outperform the least-square parameters in regression analysis. Therefore, the selection of the *b* value is dependent on the application.

8.2 Advanced empirical magnitude probability functions

The M–A algorithm is a single-parameter function. As far as a single-parameter function is concerned, its performance in simulating earthquake magnitude distributions is considered satisfactory. However, we will not be surprised by the arrivals of other functions, probably with multiple parameters, outperforming this single-parameter algorithm in the modeling of magnitude probability distributions. The bottom line is, when better models are available, we will not hesitate to use them.

8.3 Computational simplicity

The least-square regression should be the easiest method among the three to calibrate the recurrence parameters. For the MLE approach and the new procedure, both are tedious in computations, generally requiring in-house computer codes for the analysis. But

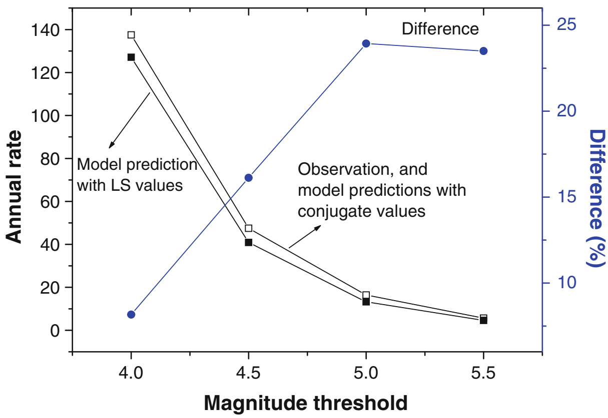

Fig. 11 With the conjugate values (i.e., MLE and the optimization method), the calculated earthquake rate can match the observation because it was used as a boundary condition in the back calculation. But when *a* value and *b* value (i.e., from LS calculation) are not conjugate, the disagreement between observation and prediction can be expected

understandably, it should be much easier to develop a computer tool for executing this straightforward procedure, in comparison with the computer program to calculate the *b* value with MLE.

8.4 Sensitivity study of *b* value in PSHA

Figure 12 shows the hazard curves for a benchmark PSHA example as mentioned previously (Kramer 1996). With *b* values increased from 0.8 to 1.0, the seismic hazard or the annual rate of ground motion decreases because of the changes in magnitude distributions (Fig. 1). For Seismic Source A, the hazard ratio using the two *b* values can be as high as 3.0 for a hazard level of PGA > 0.8 g, although basically there is no difference for PGA > 0.01 g. The same outcome was observed for Seismic Source B, with the ratio even higher (around 3.5) when the lower *b* value (=0.8) was used.

Understandably, the changes of *b* values would affect PSHA calculations, but their influence should be on a case-by-case basis, depending on other inputs such as ground motion models, maximum magnitudes, magnitude thresholds, and site locations. As a result, it is hard to propose a general picture about the influence of the *b* value on PSHA. But logically speaking, when there is a simple method available for calibrating input parameters, we will use it to improve the analysis although the result might not be too

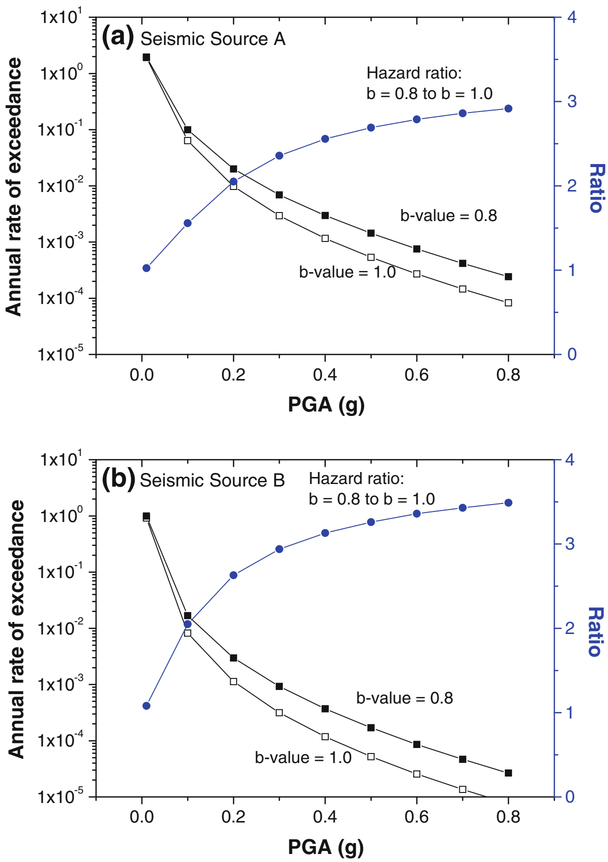

Fig. 12 Sensitivity study of *b* values on hazard curves given a benchmark PSHA example; **a** for Seismic Source A and **b** for Seismic Source B (see Fig. 1 for the respective magnitude probability distribution for the *b* values used)

different at the end. Likewise, as for the *b* value, it is a logical option for us to use the proposed method to calibrate it for PSHA studies, because it improves the modeling of observed magnitude probability distributions with a simple procedure.

9 Conclusions

This paper introduces a new approach to optimize the *b* value to fit the magnitude probability distribution calculated with the McGuire–Arabasz algorithm. The new method is simply a trial-and-error procedure, and its effectiveness was demonstrated in this paper with the earthquake data around Taiwan. More importantly, four demonstrations all show that the optimal *b* value can offer a better fit to the observed magnitude distributions than values obtained with the least-square computation and maximum likelihood estimation.

Acknowledgments The authors appreciate the reviewer's valuable comments making this article much better in many aspects on the submission. We also appreciate Editor-in-Chief Dr. Glade for his comments and efforts for the reviewing process.

References

Anbazhagan P, Vinod JS, Sitharam TG (2009) Probabilistic seismic hazard analysis for Bangalore. Nat Hazards 48:145–166

Ang A, Tang W (2007) Probability concepts in engineering: emphasis on applications to civil and environmental engineering. Wiley, New Jersey, pp 289–293

Cornell CA (1968) Engineering seismic risk analysis. Bull Seismol Soc Am 58:1583–1606

Devore JL (2008) Probability and statistics for engineering and the sciences. Duxbury Press, UK, pp 121–124

Geller RJ, Jackson DD, Kagan YY, Mulargia F (1997) Earthquake cannot be predicted. Science 275:1616

Gutenberg B, Richter CF (1944) Frequency of earthquakes in California. Bull Seismol Soc Am 34:1985–1988

Kramer SL (1996) Geotechnical earthquake engineering. Prentice Hall Inc., New Jersey, pp 116–129

McGuire RK, Arabasz WJ (1990) An introduction to probabilistic seismic hazard analysis. Geotech Environ Geophys 1:333–353

Mezcua J, Rueda J, Blanco RMG (2011) A new probabilistic seismic hazard study of Spain. Nat Hazards 59:1087–1108

Mualchin L (2005) Seismic hazard analysis for critical infrastructures in California. Eng Geol 79:177–184

Rafi Z, Lindholm C, Bungum H, Laghari A, Ahmed N (2012) Probabilistic seismic hazard of Pakistan, Azad-Jammu and Kashmir. Nat Hazards 61:1317–1354

Sokolov VY, Wenzel F, Mohindra R (2009) Probabilistic seismic hazard assessment for Romania and sensitivity analysis: a case of joint consideration of intermediate-depth (Vrancea) and shallow (crustal) seismicity. Soil Dyn Earthq Eng 29:364–381

U.S. Nuclear Regulatory Commission (2007) A performance-based approach to define the site-specific earthquake ground motion. NUREG-1.208, Washington

Wang JP, Chan CH, Wu YM (2011) The distribution of annual maximum earthquake magnitude around Taiwan and its application in the estimation of catastrophic earthquake recurrence probability. Nat Hazards 59:553–570

Wang JP, Wu YM, Lin TL, Brant L (2012a) The uncertainty of a Pd3–PGV onsite earthquake early warning system. Soil Dyn Earthq Eng 36:32–37

Wang JP, Chang SC, Wu YM, Xu Y (2012b) PGA distributions and seismic hazard evaluations in three cities in Taiwan. Nat Hazards 64:1373–1390

Wang JP, Huang D, Cheng CT, Shao KS, Wu YC, Chang CW (2013) Seismic hazard analysis for Taipei City including deaggregation, design spectra, and time history with excel applications. Comput Geosci. doi:10.1016/j.cageo.2012.09.021

Weichert DH (1980) Estimation of the earthquake recurrence parameters for unequal observation periods for different magnitudes. Bull Seismol Soc Am 70:1337–1346

Wu YM, Kanamori H (2005) Rapid assessment of damaging potential of earthquakes in Taiwan from the beginning of P waves. Bull Seismol Soc Am 95:1181–1185
Wu YM, Kanamori H (2008) Development of an earthquake early warning system using real-time strong motion signals. Sensors 8:1–9